JOURNAL OF SPACECRAFT AND ROCKETS
Vol. 54, No. 5, September–October 2017

Engineering Notes

Steady-State Attitude and Control Effort Sensitivity Analysis of Discretized Thruster Implementations

John Alcorn,* Hanspeter Schaub,† and Scott Piggott‡
University of Colorado Boulder, Boulder, Colorado 80309

DOI: 10.2514/1.A33709

Nomenclature

$\mathcal{B}$	=	body reference frame
$F_{\text{actual}}/F_{\text{nom}}/F_{\text{bias}}$	=	actual/nominal/bias force, N
I	=	moment of inertia, kg · m^2
K	=	proportional feedback gain
ℓ	=	duty cycle
$\mathcal{N}$	=	inertial reference frame
P	=	derivative feedback gain
r_t	=	thruster moment arm, m
T_p	=	pulse duration, s
$u_{\text{des}}/u_{\text{max}}$	=	desired torque/maximum torque, N · m
α	=	angular acceleration, rad/s^2
β_{p2p}	=	pulse-to-pulse repeatability
$\gamma_f/\gamma_d/\gamma_{\text{rem}}$	=	fractional/discretized/remainder pulse duration ratio
Δt	=	control update period, s
δF_{p2p}	=	pulse-to-pulse repeatability force deviation
θ	=	angle between $\mathcal{B}$ frame and $\mathcal{N}$ frame, rad
τ	=	torque, N · m
ω	=	angular velocity, rad/s

I. Introduction

HOLDING a fixed attitude with a spacecraft is often achieved using reaction wheels or control moment gyroscopes, while thrusters are used as a means of coarse pointing or performing momentum management. However, with recent advancements in thrusters and microthrusters, spacecraft designers are increasingly considering using thrusters for fine pointing [1,2]. Unlike reaction wheels, on/off thrusters may not in general be used to implement a continuous control law due to the fact that they are not able to produce incremental levels of force [3]. If a large attitude maneuver is required, an open-loop bang/bang control solution that meets the thruster firing requirements can be found (see [4] p. 32). For other scenarios such as a sun-pointing maneuver to remain power positive or inertial Earth-pointing maneuvers, a continuous control is preferred to robustly reject unmodeled disturbances. However, note that these two sample maneuvers have very different pointing and fuel usage concerns. For a short-duration Earth-pointing mode, fuel usage can be sacrificed to achieve the desired tight pointing to align the antenna at Earth. In contrast, the sun-pointing maneuver does not have strict pointing requirements but is very concerned with the long-term fuel usage to hold a power-positive orientation. The pointing requirements of a maneuver strongly dictate which actuation algorithm and corresponding performance metrics are desirable.

A continuous control law may be implemented on a configuration of thrusters in a discrete fashion without simply using a bang/bang control law [5]. Although the nominal magnitude of thrust pulse (pulse height) is constant in general, the temporal characteristics of the thrust pulse may be modulated. It is well established that when using thrusters for spacecraft attitude control pseudolinear behavior may be achieved by using pulse-width pulse-frequency modulation (PWPF) or pulse-duration modulation (PDM) [3,6] rather than bang/bang control. McClelland [7] shows extensively that PWPF modulation consistently performs better than bang/bang control or time-optimal bang/bang control based on propellant usage, implements smoother control action, and more closely approximates a linear controller. Furthermore, it is demonstrated that by avoiding the nonlinear behavior of a bang/bang controlled system excitation of resonant frequencies of the spacecraft is commonly avoided [8–10]. A patent describes attitude control using the PWPF modulation thruster control scheme and methods of hardware implementation [11].

A fundamental set of problems not covered by previous openly published literature is the limitations imposed by flight electronics on thruster-based attitude control solutions. In general, a thruster-based control system is further discretized due to the temporal resolution of the pulse time command and minimum impulse bit/minimum pulse on time. That is, any pulse-duration command given to a thruster must be greater than or equal to the minimum pulse time (dictated by how fast the thruster can open/close its main valve) and must also be a multiple of the pulse time resolution (dictated by the characteristics of the flight computer and electronics associated with the thruster). These limitations mean that a linear controller will give pulse-duration commands that cannot be applied due to the pulse-duration command either being less than the minimum pulse duration or not being an integer multiple of the pulse-duration resolution. Therefore, a pulse-duration command must be rounded up, down, or to the nearest multiple of the pulse-duration resolution in order to be applied. In addition, a simple mathematical algorithm for tracking residual (partial/unimplemented) thrust pulses is investigated to study how it may reduce the steady-state error without impacting the desired closed-loop response characteristics. Performance of the Schmitt trigger, a dual-level comparator with hysteresis, is investigated in order to compare results of the four rounding algorithms to this commonly used algorithm.

This paper presents Monte Carlo and parameter sweep simulation results of a general one-dimensional spacecraft attitude control problem involving multiple thrusters that operate in a discrete on/off fashion using PDM and different pulse rounding algorithms, including the residual tracking method, and the Schmitt trigger algorithm. In each set of simulation results, some parameters are kept fixed or swept in order to best visualize the underlying trends. Although these thruster implementation methods considered have been studied individually for a particular mission, very little is published in the open literature on the performance tradeoff between them. Rather, this overview study provides novel comprehensive insight into their relative benefits and drawbacks using a benchmark pointing problem independent of a particular mission. Consideration

Received 15 July 2016; revision received 2 February 2017; accepted for publication 7 May 2017; published online 13 July 2017.

*Graduate Research Assistant, Department of Aerospace Engineering Sciences, Colorado Center for Astrodynamics Research (CCAR). Student Member AIAA.

†Alfred T. and Betty E. Look Professor of Engineering, Department of Aerospace Engineering Sciences, 431 UCB, Colorado Center for Astrodynamics Research, Boulder, CO 80309-0431. Associate Fellow AIAA.

‡ADCS Integrated Simulation Software Lead, Laboratory for Atmospheric and Space Physics. Member AIAA.

is given to the performance of each rounding algorithm and residual tracking vs a control law that includes an integral gain. This analysis investigates how the use of integral feedback (which in linear control is implemented to accelerate convergence to zero error and cancel any static bias in error) may alter the closed-loop pointing performance and fuel usage. The performance of each algorithm and each algorithm with the introduction of an integral term are analyzed under uncertain thruster behavior by simulating an unmodeled static bias in the magnitude of the thrust pulse height. The sensitivity of each thrust pulse timing characterizing parameter is explored by showing a change in steady-state pointing accuracy as the minimum pulse duration and pulse-duration resolution are varied. The Schmitt trigger algorithm is further analyzed to show the tradeoff between the pointing performance, fuel usage, and thruster fire count for a range of comparator level combinations. Lastly, the performance of the Schmitt trigger, pulse rounding algorithms, and residual tracking algorithm are directly compared in order to identify situations (such as Earth pointing, sun pointing, and fine pointing) in which each may be applicable. The body of the paper gives details on the mathematical model, control algorithms, and numerical simulation and draws conclusions on the results.

II. Problem Statement

A one-dimensional spacecraft model with a cluster of four thrusters is used as illustrated in Fig. 1. The thruster pairings allow for pure torque couples to be generated about the vertical axis in the positive and negative senses. The control goal is always to drive the body frame orientation $\mathcal{B}$ to be equal to the inertial frame $\mathcal{N}$.

A. Equations of Motion

Without loss in generality, this study focuses on the fixed axis rotation case to investigate how discrete thruster implementation issues impact the steady-state fine pointing ability. The kinematic differential equation assumes the simple form

$$\alpha = \frac{\mathrm{d}\omega}{\mathrm{d}t} = \frac{\mathrm{d}^2\theta}{\mathrm{d}t^2} \tag{1}$$

where α is the angular acceleration, ω is the angular velocity, and θ is the angle between the spacecraft frame and the inertial frame $\mathcal{N}$ (see [12] p. 6). Each of these parameters is taken about the normal axis of the spacecraft. The dynamics of the system are governed simply by

$$\alpha = \frac{\tau}{I} \tag{2}$$

where τ is the sum of the torques applied by the thrusters and I is the inertia of the spacecraft about the axis directed out of the page (see [3] p. 510). The one-dimensional spacecraft motion allows the simulation results to be presented in a straightforward and concise manner, without loss of generality in the steady-state pointing error and associated control effort discussion.

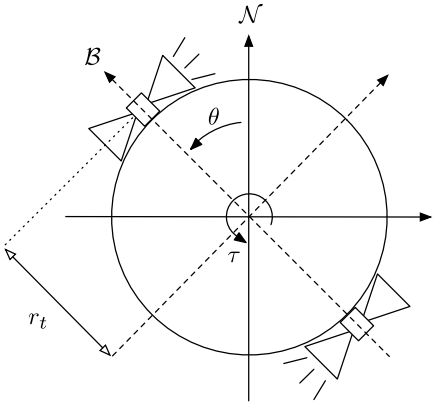

Fig. 1 A simplified spacecraft with thrusters.

B. Thruster Model

Thruster modeling errors must consider pulse-to-pulse repeatability. This is a small deviation from the nominal force a thruster produces. Pulse-to-pulse repeatability typically decreases (improves) as the thruster warms up to thermal steady-state and the valves operate more consistently between consecutive pulses. For the scope of this study, temporal variation of pulse-to-pulse repeatability is not implemented, as the additional disturbance caused by this effect is considered to be encapsulated within a conservative estimate of β_{p2p}. These characteristics vary from thruster to thruster and can certainly be difficult to model accurately. Many thruster manufacturers do provide data on pulse-to-pulse repeatability, but implementing a specific repeatability of the pulse duration curve in the model would show results specific to that thruster, which is not desirable.

In addition to pulse-to-pulse repeatability, a thruster may have a static thrust bias, causing it to fire either slightly hot or cold. The equation describing the actual thrust produced by a thruster is

$$F_{\text{actual}} = F_{\text{nom}} + F_{\text{bias}} + \delta F_{p2p} \tag{3}$$

where F_{nom} is the nominal force produced, F_{bias} is the static bias force (i.e., the thruster is stronger or weaker than expected), and δF_{p2p} is the deviation caused by pulse-to-pulse repeatability, where

$$\delta F_{p2p} \sim \mathcal{N}(0, \sigma_{p2p}^2) \tag{4}$$

It is assumed that the specified pulse-to-pulse repeatability β_{p2p} represents the fraction of max thrust equivalent to the 3σ value of δF_{p2p}. Thus, the standard deviation of the disturbance δF_{p2p} is given by

$$\sigma_{p2p} = \frac{1}{3}\beta_{p2p} F_{\text{nom}} \tag{5}$$

$$0 < \beta_{p2p} \tag{6}$$

Without loss in generality, it is assumed that each thruster is perpendicular to its moment arm with the spacecraft center of mass. Thus, torque applied to the spacecraft by each thruster is given by

$$\tau_{\text{actual}} = r_t \cdot F_{\text{actual}} \tag{7}$$

where r_t is the separation of the thruster from the center of mass of the spacecraft.

C. Control Implementation

For the research presented, the simplified spacecraft under consideration is controlled using a proportional-integral-derivative control law (see [13] p. 295). The controlled parameter is the angle θ. The control torque is given by

$$u_{\text{des}} = -K\theta_{\text{err}} - P\omega - K_i \int \theta_{\text{err}} \cdot \mathrm{d}t \tag{8}$$

where K is the proportional gain, P is the derivative gain, and K_i is the integral gain. The angle error θ_{err} is given by

$$\theta_{\text{err}} = \theta - \theta_{\text{ref}} \tag{9}$$

where θ_{ref} is the constant reference angle. Since the thrusters under consideration use PDM, the the desired torque u_{des} must be translated to a pulse duration (see [14], p. 25). The level of thruster activity relative to maximum ℓ is related to u_{des} by the equation

$$\ell = \left|\frac{u_{\text{des}}}{u_{\max}}\right| = \left|\frac{u_{\text{des}}}{r_t \cdot F_{\text{nom}}}\right| = \frac{T_p}{\Delta t} \tag{10}$$

Here, T_p is the desired pulse duration, and Δt is the control update period. Because ℓ is equivalent to the duty cycle, it must satisfy

$$0 \le \ell \le 1 \tag{11}$$

Rearranging Eq. (10) to express the pulse duration as a function of u_{des} yields

$$T_p = \ell \cdot \Delta t = \left| \frac{u_{\text{des}}}{r_t \cdot F_{\text{nom}}} \right| \cdot \Delta t \tag{12}$$

T_p represents the desired duration of the thrust pulse. Equation (10) shows that by applying a force F_{nom} for duration T_p at a frequency of $1/\Delta t$ the average torque on the spacecraft is equivalent to a case in which pulse height modulation was applied. Equivalently, the total angular momentum imparted on the system is the same in each case. Thus, the most significant difference in performance is the pseudolinear behavior of pulse duration modulation compared to continuous linear behavior of pulse height modulation.

D. Discrete Implementations

The previous section shows that a desired torque may be translated to a pulse duration T_p in order to operate thrusters using PDM. Any pulse time command given to a thruster must be greater than or equal to the minimum pulse time T_{min}, which is dictated by how fast the thruster can open/close its valve. Any pulse time must also be a multiple of the pulse time resolution T_{res}, which is dictated by the characteristics of the flight computer and electronics associated with the thruster. Thus, T_p is discretized in order to be applied to a thruster. Define γ_f as the fractional ratio of the desired pulse duration and pulse duration resolution T_{res}:

$$\gamma_f = \frac{T_p}{T_{\text{res}}} \tag{13}$$

This ratio is generally not a whole number. Consequently, to implement an integer number of pulses, γ_f must be rounded in some way. Four methods of rounding are investigated: FLOOR, ROUND, CEIL, and the pulse residual tracking method REM. The dual-level comparator Schmitt trigger allows for comparison with a commonly used algorithm that does not operate on the timing parameters T_{min} and T_{res}. Algorithm 1 shows the FLOOR method of rounding γ_f to obtain an applied pulse duration T_{on}. Using this algorithm, noninteger desired pulse ratios are always rounded down. If the desired pulse duration is less than the minimum pulse duration, T_{on} is rounded down to zero, and the thruster does not fire for the current control period.

Algorithm 2 shows the ROUND method of rounding γ_f to obtain T_{on}. Using this algorithm, noninteger desired pulse ratios are always rounded to the nearest integer. If the desired pulse duration is greater than half the minimum pulse duration, T_{on} is rounded up to T_{min}. If the desired pulse duration is less than half the minimum pulse duration, T_{on} is rounded down to zero.

Algorithm 3 shows the CEIL method of rounding γ_f to obtain T_{on}. Using this algorithm, noninteger desired pulse ratios are always rounded up. Desired pulse duration values less than T_{min} are always rounded up to T_{min}. Consequently, this algorithm inherently has issues with chatter about zero error without an applied deadband.

Algorithm 4 shows the REM method of processing γ_f to obtain T_{on}. This algorithm also tracks unimplemented thrust by retaining partial thrust pulses γ_{rem}. Using this algorithm, noninteger desired pulse ratios are always rounded down. The fractional pulse is retained for the next call to the algorithm. Desired pulse duration values less

Algorithm 1 Discrete Thrust Pulsing Using FLOOR

1: **Data:** γ_f, T_{min}, T_{res}
2: **Result:** T_{on}
3: $\gamma_d = \text{floor}(\gamma_f)$
4: **if** $\gamma_d \cdot T_{\text{res}} < T_{\text{min}}$, **then**
5: $\quad T_{\text{on}} = 0$
6: **else**
7: $\quad T_{\text{on}} = \gamma_d \cdot T_{\text{res}}$
8: **end**

Algorithm 2 Discrete thrust pulsing using ROUND

1: **Data**: γ_f, T_{min}, T_{res}
2: **Result**: T_{on}
3: $\gamma_d = \text{round}(\gamma_f)$
4: **if** $\gamma_d \cdot T_{\text{res}} < T_{\text{min}}$, **then**
5: $\quad T_{\text{on}} = \text{round}((\gamma_d \cdot T_{\text{res}})/T_{\text{min}}) \cdot T_{\text{min}}$
6: **else**
7: $\quad T_{\text{on}} = \gamma_d \cdot T_{\text{res}}$
8: **end**

Algorithm 3 Discrete thrust pulsing using CEIL

1: **Data**: γ_f, T_{min}, T_{res}
2: **Result:** T_{on}
3: $\gamma_d = \text{ceil}(\gamma_f)$
4: **if** $\gamma_d \cdot T_{\text{res}} < T_{\text{min}}$, **then**
5: $\quad T_{\text{on}} = T_{\text{min}}$
6: **else**
7: $\quad T_{\text{on}} = \gamma_d \cdot T_{\text{res}}$
8: **end**

Algorithm 4 Discrete thrust pulsing using residual tracking

1: **Data**: γ_f, γ_{rem}, T_{min}, T_{res}
2: **Result**: T_{on}
3: $\gamma_c = \gamma_f + \gamma_{\text{rem}}$
4: $\gamma_d = \text{floor}(\gamma_c)$
5: $\gamma_{\text{rem}} = \gamma_f + \gamma_{\text{rem}} - \gamma_d$
6: **if** $\gamma_d \cdot T_{\text{res}} < T_{\text{min}}$, **then**
7: $\quad T_{\text{on}} = 0$
8: $\quad \gamma_{\text{rem}} = \gamma_{\text{rem}} + \gamma_d$
9: **else**
10: $\quad T_{\text{on}} = \gamma_d \cdot T_{\text{res}}$
11: **end**

Algorithm 5 Discrete thrust pulsing using the Schmitt trigger

1: **Data**: ℓ, ℓ_{on}, ℓ_{off}, S_{last}
2: **Result**: S
3: **if** $\ell \ge \ell_{\text{on}}$, **then**
4: $\quad S = 1$ (on state)
5: **else if** $\ell \le \ell_{\text{off}}$, **then**
6: $\quad S = 0$ (off state)
7: **else**
8: $\quad S = S_{\text{last}}$ (previous state)
9: **end**

Table 1 Nominal simulation parameters for the simple spacecraft

Parameter	Value
Inertia I, kg · m^2	800
Control period Δt, s	0.5
Proportional gain K	17.5580
Derivative gain P	213.3333
Integral gain K_i	0.2
Servo rate, Hz	100
Nominal thrust F_{nom}, N	2.56
Moment arm r_t, m	1
Pulse duration resolution T_{res}, ms	10
Minimum pulse duration T_{min}, ms	20
Pulse-to-pulse repeatability β_{p2p}, %	5

Table 2 Monte Carlo simulation parameters for the integral gain sweep

Parameter	Value(s)
Integral gain K_i	0–1
Monte Carlo runs each method	220

than $T_{\min}$ are always rounded up to zero, and the fractional pulse is retained.

Algorithm 5 shows the Schmitt trigger method of discrete thrust pulsing [15–18]. The Schmitt trigger uses a dual comparator and includes hysteresis by maintaining the previous commanded thruster state. Instead of opperating on the pulse duration ratio γ_f, the Schmitt trigger uses the desired duty cycle ℓ to command a thruster state S of 1 (on) or 0 (off). Thus, T_{res} and $T_{\min}$ are not considered in the Schmitt trigger algorithm. However, these parameters still act as pulsing constraints. A pulse duration less than $T_{\min}$ may not be implemented, and pulse duration will inherently be implemented as an integer multiple of T_{res}. The Schmitt trigger uses two static comparison levels ℓ_{on} and ℓ_{off} to command a thrust state. Any desired duty cycle ℓ greater than ℓ_{on} results in the algorithm commanding an on state, whereas a desired duty cycle ℓ less than ℓ_{off} results in the algorithm commanding an off state. The algorithm implements hysteresis since

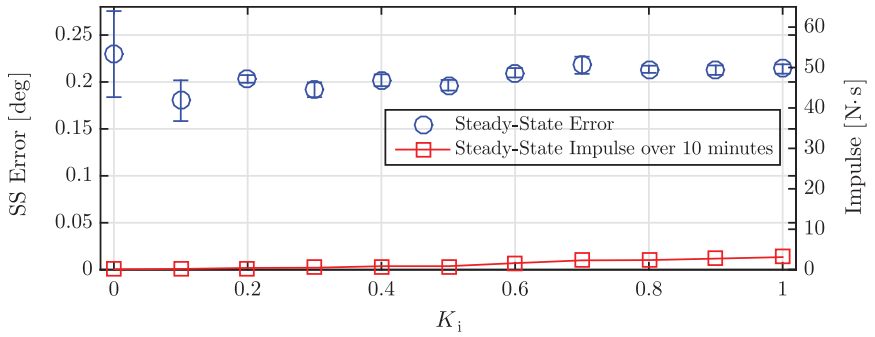

a) K_i sweep using the FLOOR pulse rounding method

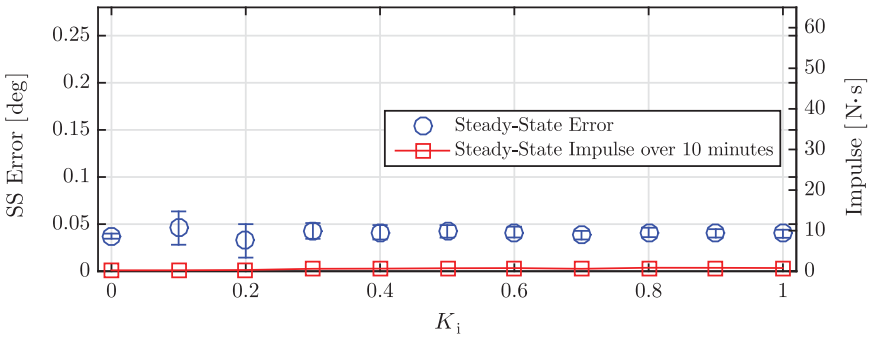

b) K_i sweep using the ROUND pulse rounding method

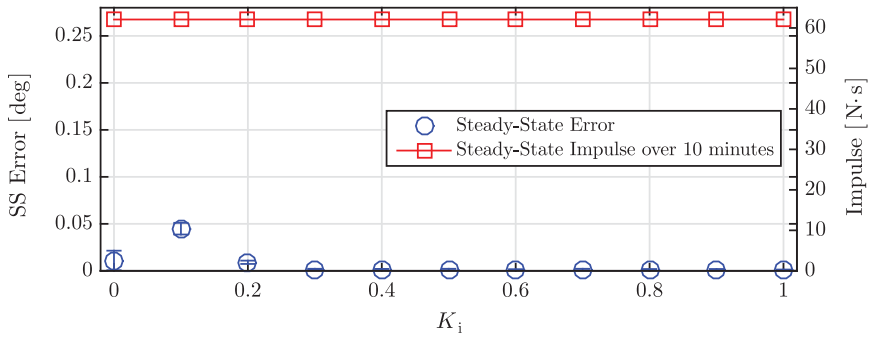

c) K_i sweep using the CEIL pulse rounding method

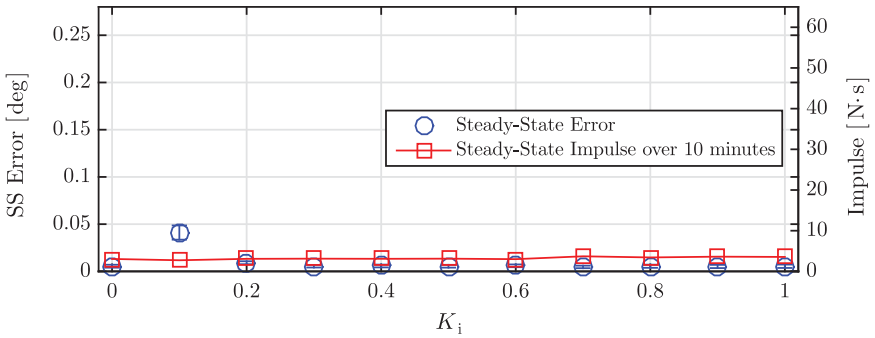

d) K_i sweep using the REM pulse rounding method

Fig. 2 Results of the integral gain sweep analysis for each algorithm (SS, steady state).

the commanded state will remain the same between control periods if one of these conditions is not met. A desired duty cycle ℓ such that $\ell_{\text{off}} \leq \ell \leq \ell_{\text{on}}$ results in the previous commanded state S_{last} being recommanded. Note that the comparator levels must be selected such that

$$\ell_{\text{off}} \leq \ell_{\text{on}} \tag{14}$$

where the special case $\ell_{\text{off}} = \ell_{\text{on}}$ resembles certain characteristics of a modified ceiling algorithm. In the case in which $\ell_{\text{off}} = 0$ and ℓ_{on} is infintesimal, the Schmitt trigger closely resembles the ceiling algorithm and is logically equivalent if $T_{\text{min}} = \Delta t$.

III. Numerical Analysis

The performance of Algorithms 1–5 is analyzed through numeric simulations using the fixed-axis rotation spacecraft model. Analyses considered include an integral gain sweep, disturbance sensitivity, and parameter sensitivity. All simulations are run in a quasi-Monte Carlo fashion in order to obtain results that represent a span of initial angles. More specifically, the initial angle is randomized, while other parameters are varied in a sweep. Underlying trends of performance metrics are extremely difficult to extract from the data when performing a multidimensional Monte Carlo analysis. Thus, for this study, only one or two parameters are varied per simulation set. Table 1 shows the nominal values for parameters used in the simulation. Note that some of the parameters given in Table 1 are varied in subsequent Monte Carlo simulations.

A. Integral Gain Sweep

The purpose of the integral gain sweep simulation is to demonstrate the performance of Algorithms 1–4 under the influence of various integral gain K_i values. Introducing integral feedback may be used to improve convergence and reject a fixed external disturbance. In the context of the rounding algorithms described in the previous section, integral feedback allows steady-state errors caused by unimplemented thruster pulses to accumulate until another pulse is commanded. For example, without an integral term, the FLOOR and ROUND algorithms may reach a state of nonzero pointing error, in which case the algorithm cannot implement a pulse due to the constraint imposed by minimum pulse duration. Of interest is how such integral terms could be used to improve the steady-state pointing error due to thruster limitations and how this compares to the precision achieved with the REM method. Steady-state error and impulse (propellant usage) are used as figures of merit for each K_i sweep. Table 2 provides parameters specific to the data given for the K_i sweep Monte Carlo simulations. Note that throughout this section the number of Monte Carlo runs given corresponds to the number of permutations of the parameters being varied.

Figure 2 shows the Monte Carlo simulation results for Algorithms 1–4, respectively. In Fig. 2a, it is shown that using an integral gain with the FLOOR method improves performance in steady-state error, but at a higher propellant cost. The pointing performance of FLOOR may be slightly improved with negligible increase in fuel usage at small values of K_i. Additionally, FLOOR is inferior to ROUND in terms of pointing performance with roughly equivalent fuel usage regardless of whether an integral term is included. Figures 2b and 2d show that the ROUND and REM algorithms are largely insensitive to the inclusion of a K_i gain. This conclusion may not be general for the ROUND algorithm, since undesired bias in steady-state error is sure to arise at higher values of T_{min}. The CEIL integral gain sweep in Fig. 2c shows that pointing performance may be slightly improved by using an integral gain. Thus, with the exception of the FLOOR algorithm (which is inferior to ROUND), it is concluded that the introduction of integral feedback does not generally improve pointing performance and may cause greater fuel usage. In Figs. 2c and 2d, a larger steady-state error at a K_i value of 0.1 is due to slower convergence (i.e., the the system oscillates about zero error).

Table 3 Monte Carlo simulation parameters for the static bias sweep

Parameter	Value, s
Static bias F_{bias}, % of max thrust	−90 to 280
Monte Carlo runs each method	260

B. Disturbance Sensitivity

The purpose of the disturbance sensitivity analysis is to show the performance of each algorithm, and each algorithm with K_i influence as an unaccounted for thrust bias is applied to a thruster. Bias of nominal thruster pulse magnitude is a common issue in spacecraft design, although it is poorly documented due mainly to the propietary characteristics of this type of information. A thruster may tend to fire more "hot or cold" over its lifetime due to a number of reasons not discussed here. Including an integral term is investigated due to its inherent ability to deal with bias in closed-loop control. For this analysis, static bias in nominal thrust pulse magnitude is allowed to vary between −90% (extremely cold) and 280% (extremely hot). Table 3 provides parameters specific to the data given for the bias sweep Monte Carlo simulations.

Figures 3 and 4 show the results of the static bias sweep simulations. Figure 3 provides a comparison of the results for all methods. Note that the FLOOR and ROUND algorithms are largely insensitive to a thruster force bias. At extremely cold biases, ROUND using integral feedback shows improved performace in mean pointing accuracy and a smaller standard deviation. The CEIL and REM algorithms show degradation in pointing performance as a bias is added. However, when using a integral gain with CEIL, the impact on performance is not as severe. Note that the REM algorithm using the integral is omitted from Fig. 4d since it shows poorer performance in certain regimes. Figure 4 shows the same data as Fig. 3 in greater detail. We conclude that FLOOR or ROUND may be desirable when static bias in nominal pulse magnitude is expected to vary and that CEIL or REM used with an integral term may be desirable when hot static bias is expected. Disturbance sensitivity results for the Schmitt trigger algorithm are not shown here since this algorithm closely resembles the ROUND algorithm.

C. Parameter Sensitivity

The purpose of the parameter sensitivity analysis is to show the performance of each algorithm as minimum pulse duration T_{min} and

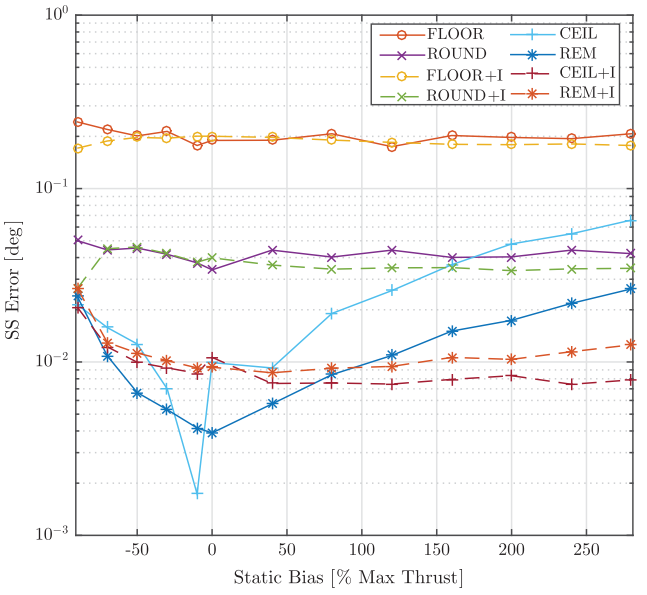

Fig. 3 Static bias sweep showing results for all methods. Dashed lines indicate the use of an integral term.

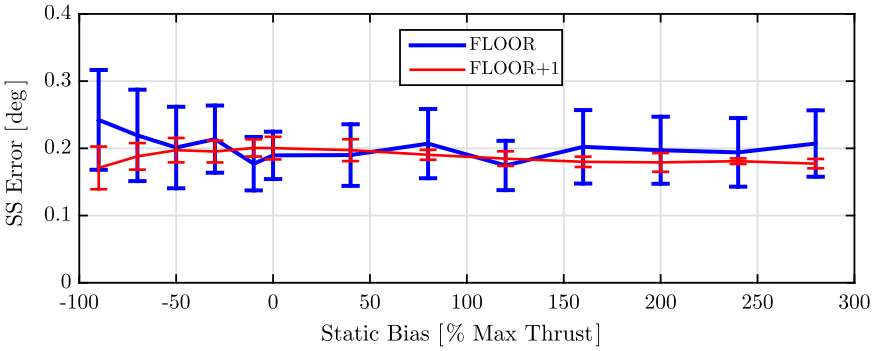

a) Static bias sweep for the FLOOR pulse rounding method

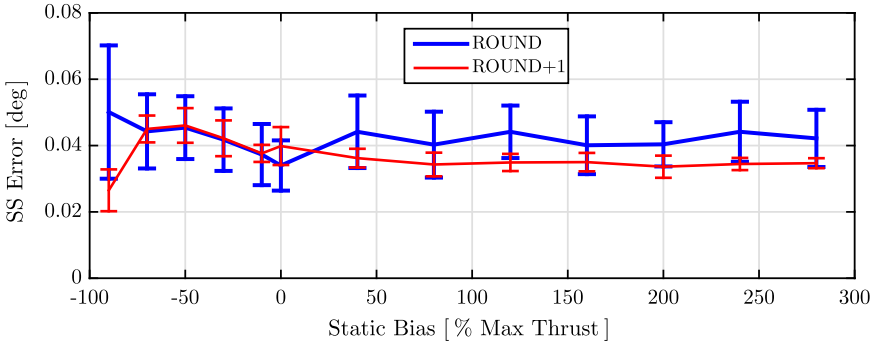

b) Static bias sweep for the ROUND pulse rounding method

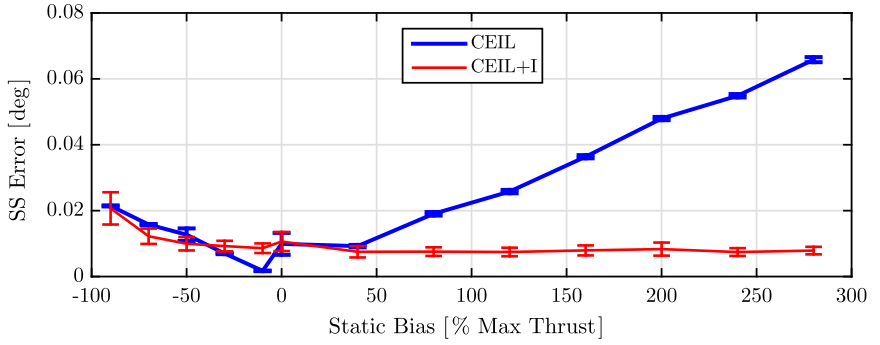

c) Static bias sweep for the CEIL pulse rounding method

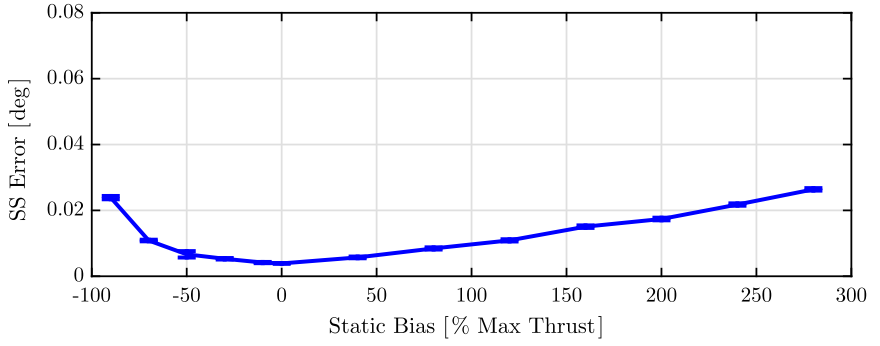

d) Static bias sweep for the REM pulse rounding method

Fig. 4 Results of the static bias sweep analysis for each algorithm.

pulse duration resolution T_{res} are varied. These parameters may not typically be changed on the fly to accomodate the desired performance. The analysis presented in this section may thus be used to compare and contrast the performance between algorithms for specific values of the timing parameters and to influence design decisions that may concern the timing parameters (commandable rate of thruster, pulse rise and fall time, minimum pulse duration, etc.). Table 4 provides parameters specific to the data given for the bias sweep Monte Carlo simulations. Figure 5 shows heat maps of steady-state error for each of the four rounding algorithms and the Schmitt trigger. From the data, it is easy to infer that steady-state error is highly correlated with T_{min} for the FLOOR, ROUND, and REM methods. The main difference between the algorithms is sensitivity to T_{res}. Figure 5a suggests that the FLOOR method shows a small

Table 4 Monte Carlo simulation parameters for the parameter sensitivity sweep

Parameter	Value(s)
Minimum pulse duration T_{min}, ms	0–500
Pulse duration resolution T_{res}, ms	0–500
Monte Carlo runs each method	160

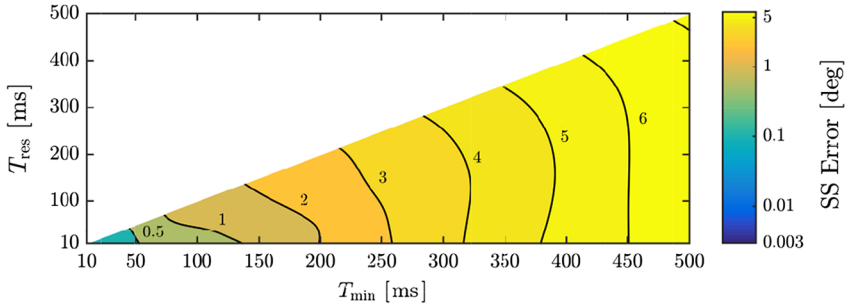

a) Static bias sweep for the FLOOR pulse rounding method

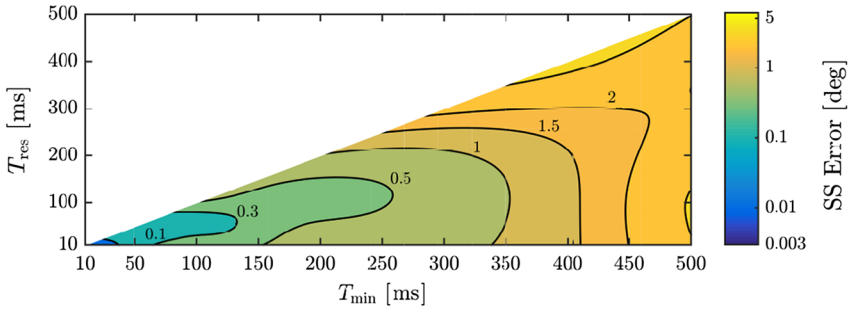

b) Static bias sweep for the ROUND pulse rounding method

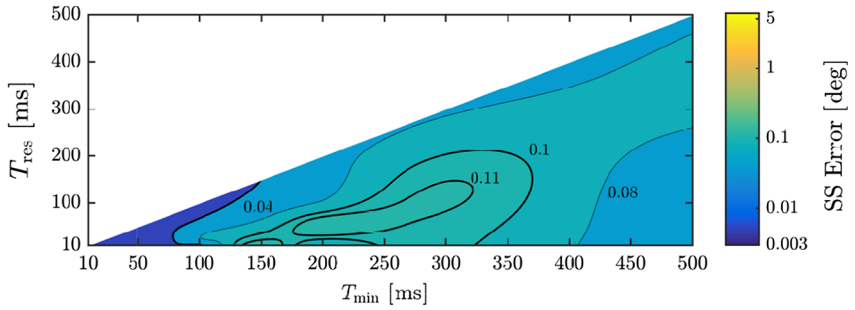

c) Static bias sweep for the CEIL pulse rounding method

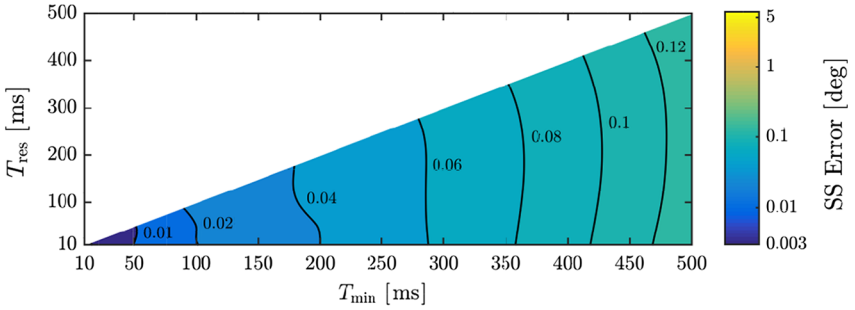

d) Static bias sweep for the REM pulse rounding method

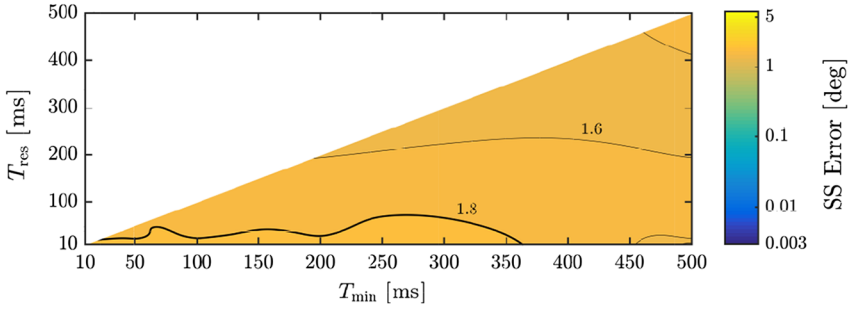

e) Static bias sweep for the Schmitt trigger algorithm with comparator values $l_{off} = 30$ and $l_{on} = 40$

Fig. 5 Steady-state pointing performance results of the parameter sensitivity analysis for each algorithm.

correlation between T_{res} and the steady-state error. Figure 5b shows that for the ROUND method the correlation between T_{res} and the steady-state error is very large at small values of T_{min} and very small at larger values of T_{min}. Figure 5c shows that the CEIL algorithm is largely insensitive to T_{res} over the range of values considered. Figure 5d shows that the REM algorithm is largely insensitive to T_{res}.

Table 5 Monte Carlo simulation parameters for the Schmitt trigger comparator sweep

Parameter	Value(s)
Schmitt on level ℓ_{on}, %	4–98
Schmitt off level ℓ_{off}, %	2–96
Total Monte Carlo runs	2670

Figure 5e shows that the Schmitt trigger with comparator values $\ell_{off} = 30$ and $\ell_{on} = 40$ is insensitive to both T_{res} and T_{min}.

D. Schmitt Trigger Performance

Discrete thruster pulsing with the Schmitt trigger algorithm [19,20] is characterized in terms of the steady-state pointing error, steady-state fuel usage, and steady-state thruster fire count for a range of Schmitt

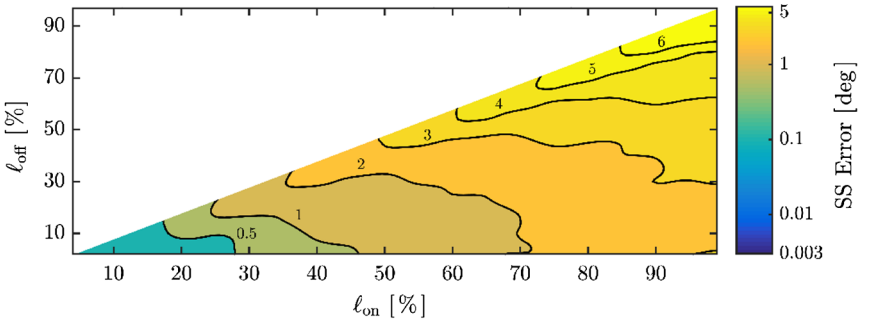

a) Steady-state pointing error vs Schmitt trigger l_{on}/l_{off} combination

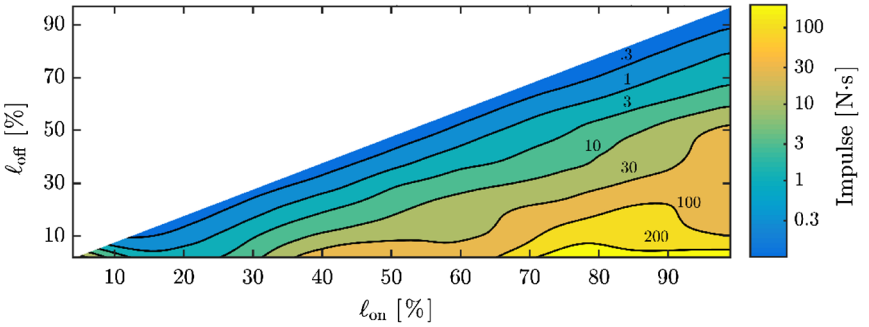

b) Steady-state impulse over 10 min vs Schmitt trigger l_{on}/l_{off} combination

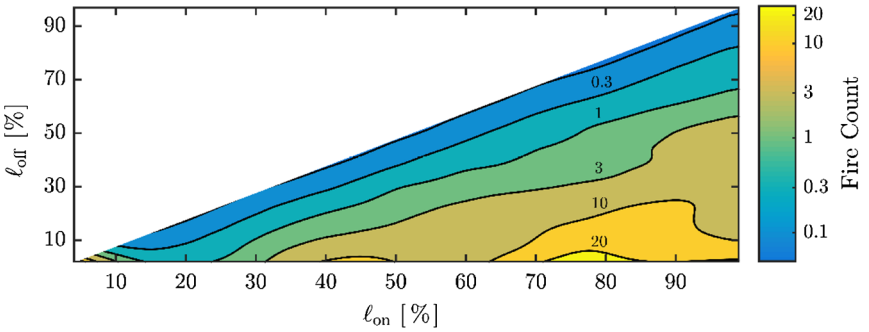

c) Steady-state thruster fire count over 10 min vs Schmitt trigger l_{on}/l_{off} combination

Fig. 6 Results of the Schmitt trigger performance analysis.

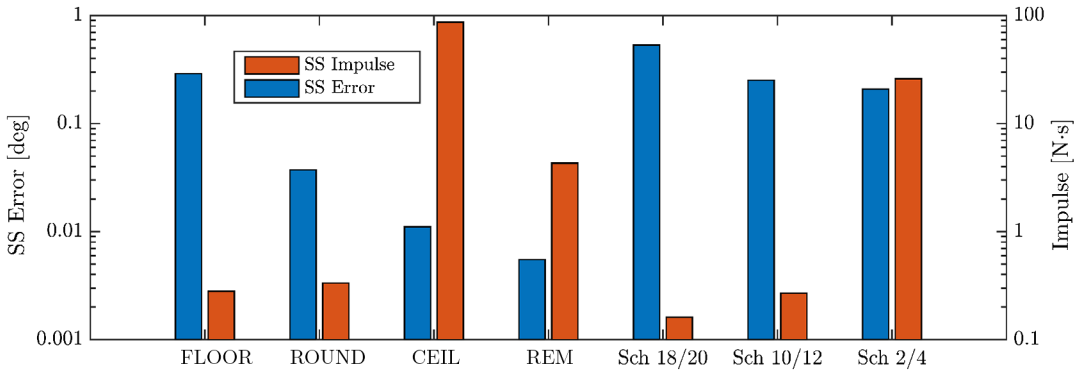

Fig. 7 Summary of results for each algorithm (Sch, Schmitt).

ℓ_{on}/ℓ_{off} combinations. This analysis serves to determine optimal choices of ℓ_{on} and ℓ_{off} for the desired performance scheme. Table 5 shows the Monte Carlo simulation parameters used for the analysis. The results of the Monte Carlo simulations are shown in Fig. 6, which shows the steady-state pointing error, impulse, and fire count for a range of Schmitt ℓ_{on}/ℓ_{off} combinations. Figure 6a shows the steady-state pointing error plotted vs a range of Schmitt on/off pairs. The clear trend in these data indicates that in general setting both ℓ_{on} and ℓ_{off} to a small value allows for an optimal steady-state pointing error. Furthermore, setting the two Schmitt comparator values to be numerically close to each other improves the pointing performance. The fact that setting the two Schmitt comparator levels close to each other or equal implies that the Schmitt trigger closely approximates a modified ROUND algorithm. Figure 6b shows the steady-state impulse (i.e., fuel usage) over a 10 min period plotted vs Schmitt comparator level combinations. This data suggest that setting ℓ_{on} and ℓ_{off} numerically close to each other will allow for better fuel usage performance. Small values of ℓ_{on} and ℓ_{off} should be avoided, though, since fuel usage tends to increase in this region. The thruster fire count, shown in Fig. 6c, shows a very similar trend. Thus, there is a tradeoff between the pointing error and fuel usage. Both sets of data show that ℓ_{on} and ℓ_{off} should be set close to each other, but fuel usage is traded for pointing accuracy as the two comparator levels are decreased. A summary of performance-related simulation results for all algorithms is shown in Fig. 7.

IV. Conclusions

The results show the performance of different methods of thruster pulse rounding for discretely operating pulse-duration modulation thrusters. Monte Carlo simulations show the sensitivity of each algorithm to an integral gain, static bias, and variation of parameters. The results show that the pulse remainder tracking algorithm REM may be used to increase steady-state pointing accuracy while maintaining much lower propellant usage than other algorithms. Although an integral feedback term does not in general improve pointing accuracy, the REM algorithm maintains its superior performance under large static thrust biases if an integral gain is introduced. The Schmitt trigger results indicate that excellent fuel usage may be achieved, without sacrificing significant pointing performance. The Schmitt trigger comparator levels may be tweaked to tune the tradeoff between the fuel usage and steady-state pointing error. However, for some comparator pairs, this algorithm becomes inferior compared to the ROUND or REM algorithms, as is demonstrated by the Schmitt trigger with comparator levels at 2%/4%. The data presented also allow us to draw general conclusions on the utility of the pulse rounding algorithms FLOOR, ROUND, and CEIL; the pulse tracking algorithm REM; and the Schmitt trigger algorithm at different comparator level combinations. Fine pointing may be achieved using the residual tracking method (such as for Earth pointing or science pointing), whereas ROUND or the Schmitt trigger provides coarse pointing at far better fuel usage (such as for sun pointing or holding some other fixed orientation without the need for fine pointing). Use of the CEIL method is not recommended for steady-state control, as it performs poorly compared to the residual tracking algorithm at a higher fuel cost.

References

[1] Katz, I., "Electric Propulsion for JPL Missions," *41st AIAA/ASME/SAE/ASEE Joint Propulsion Conference & Exhibit*, AIAA Paper 2005-3674, 2005.
doi:10.2514/6.2005-3674

[2] Köhler, J., Bejhed, J., Kratz, H., Bruhn, F., Lindberg, U., Hjort, K., and Stenmark, L., "A Hybrid Cold Gas Microthruster System for Spacecraft," *Sensors and Actuators A: Physical*, Vol. 97, 2002, pp. 587–598.

[3] Wertz, J. R., *Spacecraft Attitude Determination and Control*, Springer Science and Business Media, New York, 2012, pp. 272–277.
doi:10.1007/978-94-009-9907-7

[4] Bryson, A. E., Jr., *Control of Spacecraft and Aircraft*, Princeton Univ. Press, Princeton, NJ, 1994, pp. 32–36, Chap. 3.

[5] Dodds, S. J., and Williamson, S. E., "A Signed Switching Time Bang-Bang Attitude Control Law for Fine Pointing of Flexible Spacecraft," *International Journal of Control*, Vol. 40, No. 4, 1984, pp. 795–811.

[6] Barr, M., "Pulse Width Modulation," *Embedded Systems Programming*, Vol. 14, No. 10, 2001, pp. 103–104.

[7] McClelland, R. S., "Spacecraft Attitude Control System Performance Using Pulse-Width Pulse-Frequency Modulated Thrusters," M.S. Thesis, Naval Postgraduate School, 1994.

[8] Agrawal, B. N., McClelland, R. S., and Song, G., "Attitude Control of Flexible Spacecraft Using Pulse-Width Pulse-Frequency Modulated Thrusters," *Space Technology-Kedlington*, Vol. 17, No. 1, 1997, pp. 15–34.

[9] Agrawal, B. N., and Bang, H., "Slew Maneuver of a Flexible Spacecraft Using On-Off Thrusters," *AIAA Guidance, Navigation and Control Conference*, Vol. 1, AIAA, Washington, D.C., 1993, pp. 224–233.

[10] Song, G., Buck, N. V., and Agrawal, B. N., "Spacecraft Vibration Reduction Using Pulse-Width Pulse-Frequency Modulated Input Shaper," *Journal of Guidance, Control, and Dynamics*, Vol. 22, No. 3, 1999, pp. 433–440.

[11] Chan, F. N., and Nilsen, F. C., U.S. Patent Application for "Digital PWPF Three Axis Spacecraft Attitude Control," Docket No. 4,599,697, filed Aug. 1982, 1986.

[12] Hughes, P. C., *Spacecraft Attitude Dynamics*, Dover, New York, 2004, pp. 6–31, Chap. 2.

[13] Schaub, H., and Junkins, J. L., *Analytical Mechanics of Space Systems*, AIAA Education Series, AIAA, Reston, VA, 2014, pp. 115–158, 285–324, Chaps. 4, 8.

[14] Sun, J., "Pulse-Width Modulation," *Dynamics and Control of Switched Electronic Systems*, Springer Science and Business Media, New York, 2012, pp. 25–61, Chap. 2.

[15] Arantes, G., Martins-Filho, L. S., and Santana, A. C., "Optimal On-Off Attitude Control for the Brazilian Multimission Platform Satellite," *Mathematical Problems in Engineering*, Vol. 2009, 2009.
doi:10.1155/2009/750945

[16] Kim, J., and Kim, J., "Disturbance Accommodating Spacecraft Attitude Control Using Thruster," *AIAA/AAS Astrodynamics Conference*, AIAA Paper 1996-3663, 1996, pp. 800–805.

[17] Avanzini, G., and de Matteis, G., "Bifurcation Analysis of Attitude Dynamics in Rigid Spacecraft with Switching Control Logics," *Journal of Guidance, Control, and Dynamics*, Vol. 24, No. 5, 2001, pp. 953–959.

[18] Fleming, A. W., U.S. Patent Application for "Satellite Nutation Attenuation Apparatus," Docket No. 3,984,071, filed Aug. 1974, 1976.

[19] Anthony, T. C., Wie, B., and Carroll, S., "Pulse-Modulated Control Synthesis for a Flexible Spacecraft," *Journal of Guidance, Control, and Dynamics*, Vol. 13, No. 6, 1990, pp. 1014–1022.

[20] Romano, M., Friedman, D. A., and Shay, T. J., "Laboratory Experimentation of Autonomous Spacecraft Approach and Docking to a Collaborative Target," *Journal of Spacecraft and Rockets*, Vol. 44, No. 1, 2007, pp. 164–173.

J. A. Christian
Associate Editor